UDK: 621.454.019.2
COSATI: 21-09

Influence of Trimodal Fraction Mixture of Ammonium-Perchlorate on Characteristics of Composite Rocket Propellants

Vesna Rodić, BSc (Eng)[1)]
Miomir Bajlovski, BSc (Eng)[1)]

The examination results of composite rocket propellant composits with three different fractions of ammonium-perchlorate particle size: 200 μm, 400 μm and 80 μm and constant total solid content are presented in this paper. Burning rate and pressure exponent in the burning rate law (ballistic measures) as well as tensile strength and strain at maximum load (uniaxial mechanical characteristics) were calculated as responses according to the method of local simplex - lattice planning of the partial third series.

Key words: **composite solid propellant, ammonium-perchlorate, burning rate, exponent of burning rate, planned experiment, tensile strength, strain.**

Introduction

THE burning characteristics of solid propellants is of major significance for their use. Therefore, it is important to establish an accurate examination of propellant combustion [1]. The solid phase quantity has the greatest effect on the burning rate and by changing the oxidizer fraction ratios, the largest ranges of that response can be achieved [2]. Varying the role of some oxidizers' particle size changes the burning rate, total combustion area and effectuated pressure in the motor case. In this way, propellants with different burning rates, motor combustion time, pressure level and thermic tension of the motor case are obtained. Burning rate depends on the case pressure, working temperature and the propellant characteristics [3]. In this paper, three ammonium-perchlorate (AP) fractions have been used as oxidizers for the propellant preparation, with the mean particle diameter of 200 μm, 400 μm and 80μm.

One of the assumptions is that aluminium (Al) addition affects the propellant burning rate that it melts during the combustion while increasing the propellant surface temperature and thereby the caloric flux value from the gas phase to the solid surface. The flux increase is the conseqence of more inclined temperature gradient, enhanced termal conductivity of gasses and reduced average thermal capacity of the propellant [4]. The metal powder role is to provide the desired energy level of the propellant and contribute to combustion stability.

The chosen polymer type, along with other binder components, influences mechanical and rheological characteristics, as well as composite solid propellant's (CSP) life.

Experiment

Constant solid content propellants were examined by changing the part of three AP fractions with mean particle sizes of 200 μm, 400 μm and 80 μm [5]. The experiment was performed according to the method of local simplex - lattice planning of the partial third series. With this planning procedure, by reducing the experiment numbers, mathematical models describing the examined responses in the examination area can be obtained [6].

Selected limits of the used AP fractions are illustrated in the working matrix for real coordinates and in the plan matrix for encoded coordinates, as shown in Table 1.

Table 1: Working matrix with real values and plan matrix with encoded values

	Working matrix				Plan matrix			
granulation	label	Y_1	Y_2	Y_3	label	Y_1	Y_2	Y_3
200 μm	x_1	70	0	50	X_1	1	0	0
400 μm	x_2	0	50	0	X_2	0	1	0
80 μm	x_3	30	50	50	X_3	0	0	1

The chosen experimental area in the real system is linked to the simplex – lattice plan domain with the encoded values by determining the mathematical relations between the encoded (X_1, X_2, X_3) and real coordinates (x_1, x_2, x_3). The position of the working matrix plan with real values is given in Fig.1 and experimental domain and point positions in the plan matrix with encoded values in Fig.2.

The composition with 69 mas. % AP and 14 mas.% Al powder ($d = 5$)μm was used. Hydroxylterminated polybutadiene (HTPB) was used as a binder and toluene-diisocyanate (TDI) as a curing agent.

[1)] Military Technical Institute (VTI), Ratka Resanovića 1, 11132 Belgrade

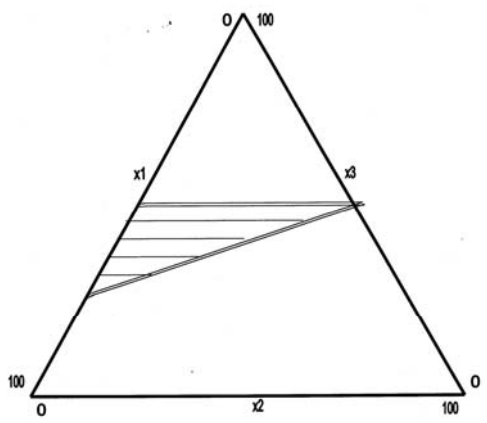

Figure 1. Plan location in the working matrix

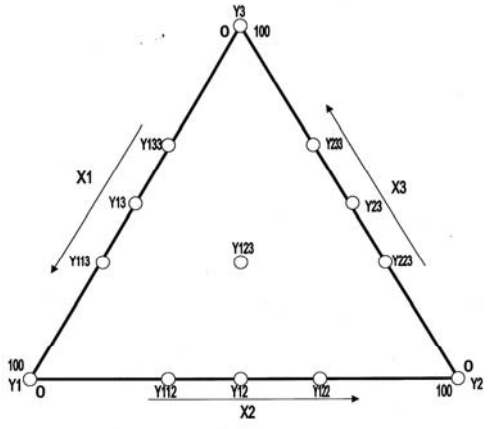

Figure 2. Matrix domain with experimental points

The fraction quantities of AP trimodal mixture for 13 formulations done according to the experiment plan are shown in Table 2.

Table 2. Fraction ratios of oxidizers according to the experiment plan

No of compo-sition	label of exp.	working matrix			mas.% AP in propellant		
		200 μm	400 μm	80 μm	200 μm	400 μm	80 μm
1	Y1	70	0	30	48.30	0	20.70
2	Y2	0	50	50	0	34.50	34.50
3	Y3	50	0	50	34.50	0	34.50
4	Y123	40.0	16.7	43.3	27.60	11.52	29.88
5	Y112*	46.9	16.5	36.6	32.36	11.38	25.26
6	Y113*	63.4	0	36.6	43.75	0	25.25
7	Y122*	23.1	33.5	43.4	15.94	23.12	29.95
8	Y133*	56.6	0	43.4	39.05	0	29.95
9	Y223*	16.5	33.5	50	11.38	23.12	34.50
10	Y233*	33.5	16.5	50	23.12	11.38	34.50
11	Y12	35	25	40	24.15	17.25	27.60
12	Y13	60	0	40	41.40	0	27.60
13	Y23	25	25	50	17.25	17.25	34.50

NOTE: * ‘ control points

The propellant compositions, including the coarse oxidizer particles, are very inconvenient from theirs packing viewpoint, so uncured propellant viscosity and density were also measured. These results were not used for mathematical modelling, but for discussing the results and are shown in Table 3.

The propellant was homogenized under vacuum at 60ºC, in the planet mixer, and cured for 120 hours at 70°C. Viscosity-time dependencies were performed at Brookfield HBT type of viscometry, at 5°/min and at 60ºC. The burning rate law was determined in the experimental motor EM 2 at 20°C. Mechanical characteristics examinations were carried out on the universal tester “INSTRON”, by uniaxial tensile testing of specimen JANAF “C” [7] at 20ºC, 50ºC and –50ºC, and the crosshead speed 50 mm/min [8]. The propellant densities were determined by Moor scale method in toluene [9].

Table 3. Viscosity and density propellant values

No.	Viscosity (Pas) after 15 min	ρ, g/cm^3
1	781	1.697
2	432	1.698
3	994	1.701
4	774	1.702
5	992	1.694
6	1235	1.696
7	1155	1.694
8	691	1.703
9	637	1.704
10	483	1.700
11	506	1.701
12	842	1.704
13	739	1.704

Results and discussion

The burning rate law parameters of CSP are shown in Table 4.

Table 4. Burning rate law parameters of CSP

Composition	v_{70}, mm/s	n	B
1	8.74	0.438	1.359
2	7.43	0.493	0.915
3	9.25	0.458	1.319
4	8.52	0.509	0.980
5	8.36	0.496	1.018
6	8.80	0.493	1.084
7	7.97	0.521	0.870
8	9.24	0.480	1.204
9	8.20	0.503	0.969
10	8.77	0.516	0.980
11	8.08	0.502	0.958
12	8.91	0.477	1.174
13	8.57	0.530	0.902

Burning rate law $V=Bp^n$
V – burning rate, mm/s,
n – exponent of pressure,
B – rate of burning at the pressure of 101.325 kPa

The results of the uniaxial tensile properties testing are given in Table 5.

Table 5. Uniaxial tensile properties values

No	50°C		20°C		-50°C	
	σ_m (MPa)	ε_m (%)	σ_m (MPa)	ε_m (%)	σ_m (MPa)	ε_m (%)
1	0.602	7.171	0.761	8.903	3.156	11.975
2	0.600	7.983	0.751	10.207	3.240	13.358
3	0.800	5.808	0.977	7.546	3.487	8.500
4	0.731	5.893	0.895	7.860	3.594	10.808
5	0.603	5.418	0.801	8.066	3.594	11.801
6	0.688	6.143	0.781	7.301	3.260	10.785
7	0.663	8.631	0.795	10.812	3.327	14.710
8	0.786	7.559	0.894	8.710	3.361	12.675
9	0.690	7.701	0.818	9.006	3.540	13.268
10	0.745	7.686	0.893	9.747	3.559	11.931
11	0.685	8.622	0.835	11.001	3.430	14.710
12	0.713	7.822	0.877	10.230	3.316	13.353
13	0.696	9.022	0.783	10.350	3.514	14.941

σ_m (MPa) – tensile stress; ε_m (%) – strain at maximum load

The results from Tables 4 and 5 are arranged by means of statistical analysis (except for the values of mechanical characteristics at extreme temperatures). Coefficients of regression were calculated for each response by applying mathematical (regression) models for the local simplex – lattice planning of the partial third series. [5], [10].

Response value calculations and model adequacy verifications were performed at control plan points (Table 2). On the basis of the attained values, the value of Student t-test was evaluated and compared with the table t-test value for the chosen reliability (α) and calculated degree freedom [10]. If the calculated t-criteria is lower than the table value, the mathematical model equation then describes the response in the adequate manner in the investigated area and the obtained dependence can be used for calculating the response at any point of the experimental plan.

Burning rate

Regression equation of the mathematical model that describes the burning rate - varying AP fraction ratio dependence is obtained.

$$Y_{v70} = 8.74X_1 + 7.43X_2 + 9.25X_3 - 0.02X_1X_2 + 0.34X_1X_3 + 0.92X_2X_3 - 0.42X_1X_2X_3 \quad (1)$$

The verification results at control points have shown that the attained model describes the burning rate in the adequate manner, as seen in Table 6.

Table 6. Adequacy verification of the burning rate model

control points	y	Y'	t_{cal}	A ($t_{cal}<t_{tab}$)
Y112	8.36	8.30	0.18	ADEQUATE
Y113	8.80	8.83	0.10	ADEQUATE
Y122	7.97	7.86	0.31	ADEQUATE
Y133	9.24	9.00	0.68	ADEQUATE
Y223	8.20	8.24	0.12	ADEQUATE
Y233	8.77	8.85	0.22	ADEQUATE
S_y=0.36mm/s	f = 7	α = 0.05	t_{tab} = 2.36	

The burning rate values at 70 bar, over encoded values, are shown in Fig.3.

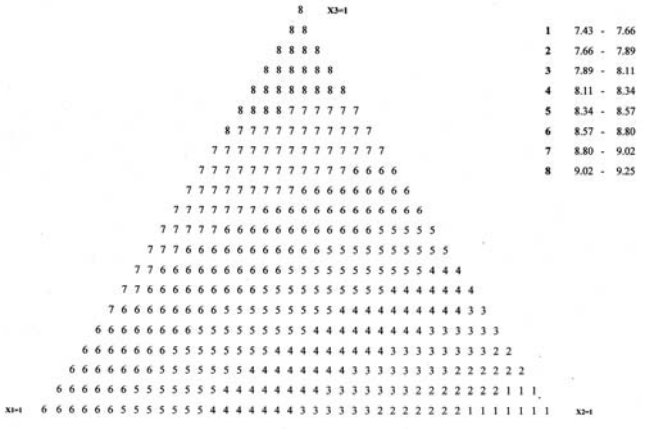

Figure 3. Burning rate levels in the plan matrix

Since large particles of AP were used in this examination, the burning rate values would be categorized as slower. For the chosen energy level composition the burning rate at 70 bar is changed from 7.4 mm/s to 9.2mm/s (25%). Besides particle sizes, burning rate also depends on the particle size ratios, i.e. on the package density. The packing mode can be represented through density and viscosity value 15 minute after the curing agent was added. Bimodal mixture consisting of 200 μm and 80 μm AP from the experiment plan can be observed as the initial system.

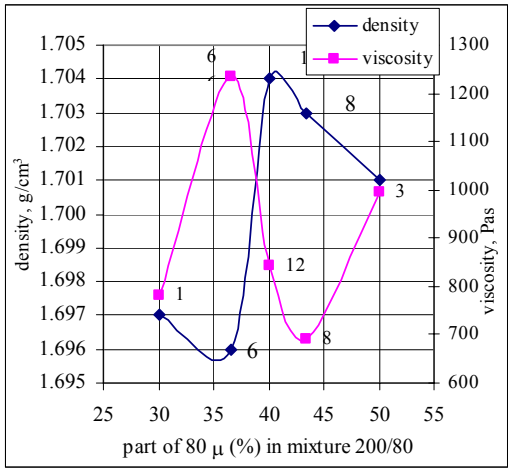

Figure 4. Effect of 80 mm AP on the density and viscosity values

There is a dependence between density i.e. viscosity values and part of 80 μm AP in the mixture. The optimum values of the densities (>1.700), viscosity (<900 Pas) and maximum burning rates from Table 4 were obtained in case of 40 mas.% or more of 80 μm AP content (compositions No.12, 8 and 3).

If mixtures of 50 mas.% of 80 μm AP are observed more closely, and the changes of the two other fractions (No.3, 10, 13 and 9) noticed, the curves in Figures 5 and 6 are obtained.

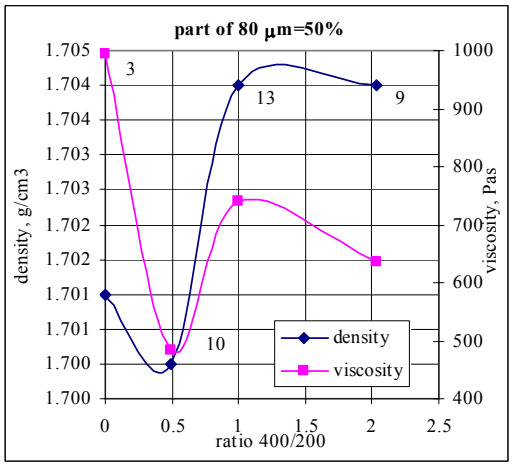

Figure 5. Effect of 400/200 ratio at mas.% 80 μm=50=const on the density and viscosity values

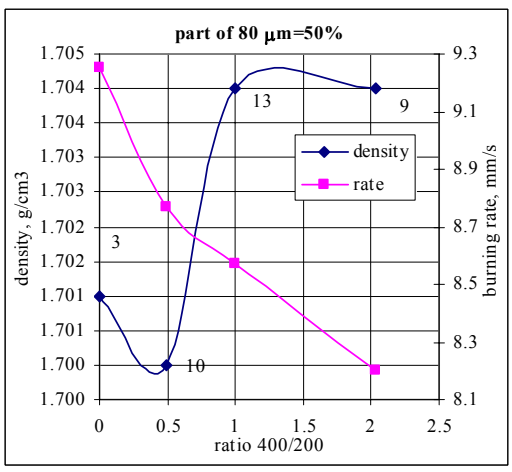

Figure 6. Effect of 400/200 ratio at mas.% 80 μm=50=const on the density and the burning rate values

Adding the third, largest fraction of AP to the mixture, density and viscosity values follow each other, as shown in Fig.5. The effect of increasing the abscise ratio, according to the free particle surfaces available reflecting in the burning rate degradation (Fig.6).

If part of the coarse fraction is kept approximately constant (16.5-16.7 mas.%), it can be seen from Fig.7 that the increase of the smallest particles (from 36.6 mas.% for No.5 to 50 mas.% for No. 10) brings about the viscosity drop for 50 % and the burning rate and density rise (Table 3).

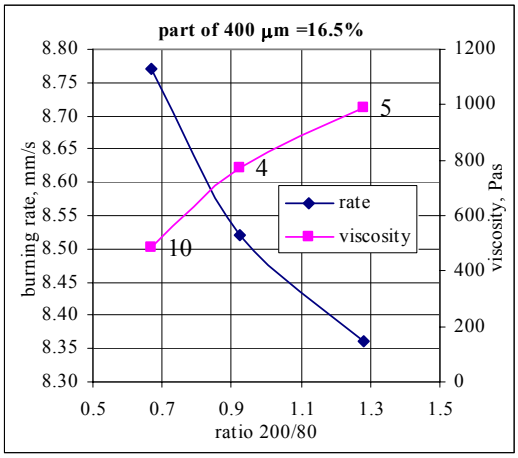

Figure 7. Effect of 200/80 ratio at mas.% 400 μm=16.5=const on the viscosity and the burning rate values

Pressure exponent in burning rate law

In the same way as for the burning rate, the regression equation of the mathematical model for pressure exponent is obtained and shown as follows:

$$Yn = 0.438X_1 + 0.493X_2 + 0.458X_3 + 0.145X_1X_2 + 0.115X_1X_3 + 0.216X_2X_3\ \ 0.194X_1X_2X_3 \quad (2)$$

The verification model results are shown in Table 7.

Table 7. Adequacy verification of the pressure exponent model

control points	y	Y'	t_{cal}	A ($t_{cal}<t_{tab}$)
Y112	0.496	0.489	0.24	ADEQUATE
Y113	0.493	0.471	0.77	ADEQUATE
Y122	0.521	0.507	0.49	ADEQUATE
Y133	0.480	0.477	0.08	ADEQUATE
Y223	0.503	0.529	0.93	ADEQUATE
Y233	0.516	0.518	0.08	ADEQUATE
S_y=0.03	f=7	α=0.05	t_{tab}=2.36	

Pressure exponents are shown via encoded values in Fig.8.

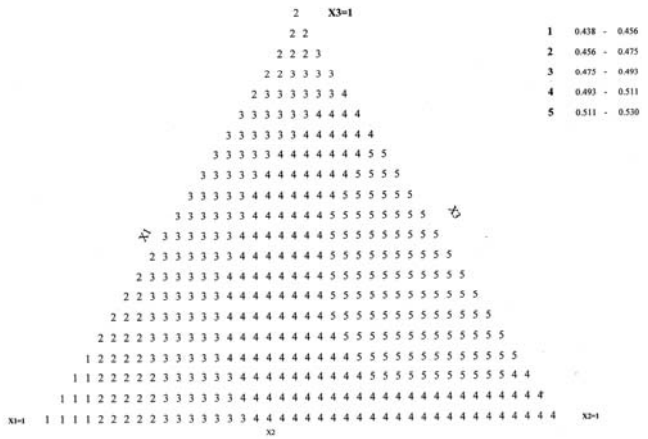

Figure 8. Pressure exponent levels in the plan matrix

The pressure exponent values range from 0.438 to 0.530 (20 %); they are classified as higher exponent values and thereby very inadequate. The lowest values are obtained for compositions without the coarsest AP fraction as seen in Fig.8, (lower left angle) and Fig.9 for bimodal mixture whereas all exponent values are below 0.48. From Fig.9 the same character for both curves can be seen.

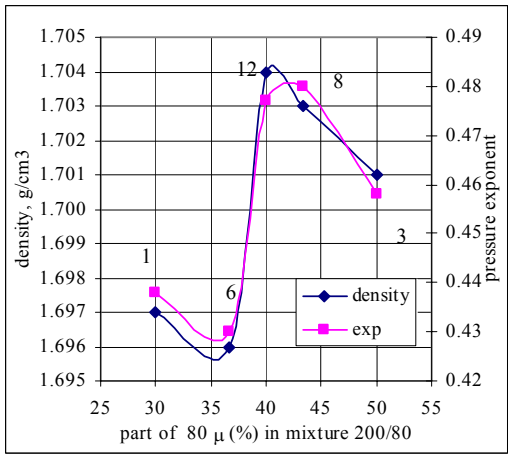

Figure 9. Effect of 80 μm AP on the density and pressure exponent values

The greatest pressure exponent values are the consequence of all three fractions, using most of 80 μm AP (Fig.10).

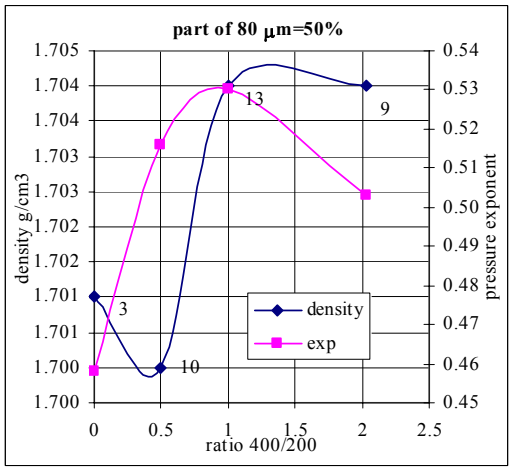

Figure 10. Effect of 400/200 ratio at mas.% 80 μm=50=const on the density and the pressure exponent values

In case of constant content of 400 μm, increase of the 200/80 ratio is followed by the rise of viscosity, while the pressure exponent falls, as shown in Fig.11.

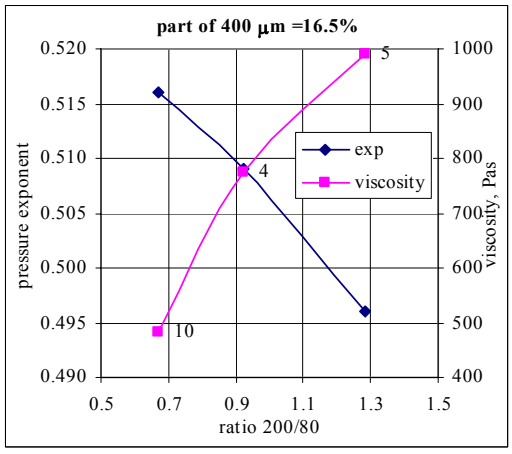

Figure 11. Effect of 200/80 ratio at mas.% 400 μm=16.5=const on the viscosity and the pressure exponent values

Tensile strength

Equation 3 is a mathematical model specifying the change of tensile strength value (σ_m) at room temperature:

$$Y_{\sigma}^{20} = 0.761X_1 + 0.751X_2 + 0.977X_3 + 0.316X_1X_2 + 0.032X_1X_3\ \ 0.324X_2X_3 + 1.692X_1X_2X_3 \quad (3)$$

The verification results of the model are shown in Table 8 and tensile strength via encoded values in Fig.12.

Table 8. Adequacy verification of the tensile strength model at 20 °C

control points	y	Y'	t_{cal}	A ($t_{cal}<t_{tab}$)
Y112	0.801	0.828	0.66	ADEQUATE
Y113	0.781	0.840	1.45	ADEQUATE
Y122	0.795	0.824	0.72	ADEQUATE
Y133	0.894	0.912	0.44	ADEQUATE
Y223	0.818	0.754	1.56	ADEQUATE
Y233	0.893	0.829	1.55	ADEQUATE
S_y=0.0425 MPa	f=7	α=0.05	t_{tab}=2.36	

Values σ_m at 20°C range from 0.75 MPa to 1 MPa (33%). The largest values are obtained for compositions without 400 μm AP fraction as seen in Figures 12 and 13 (No.3). It results from the fact that the increase in smaller fraction part is qualitatively equivalent to the expanding of oxidizer/binder free contact surface and this link becomes significantly better by adding the bonding agent. The lowest values are obtained with compositions with coarse AP particles and almost equivalent content of 400 μm and 200 μm, when free contact surfaces diminish, and so does the bonding agent. Namely, the agent reacts on a smaller surface, so the tensile strength results are adequate.

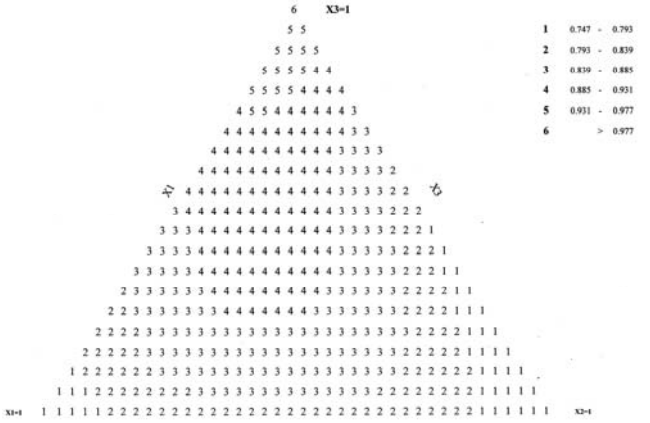

Figure 12. Tensile strength levels at 20 °C in the plan matrix

The greater content of the coarsest fraction, the greater value of viscosity (Fig.13).

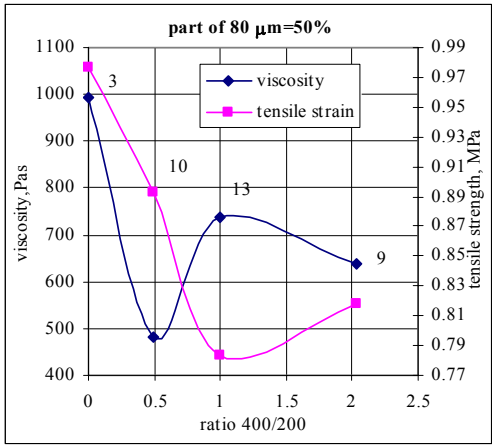

Figure 13. Effect of 400/200 ratio at mas.% 80 μm=50=const on the viscosity and the tensile strength values

Strain at maximum load

Equation 4 was derived as a mathematical model which outlines the change of strain at maximum load at room temperature.

$$Y_{\varepsilon}^{20} = 8.903X_1 + 10.207X_2 + 7.546X_3 + 5.784X_1X_2 + 8.022X_1X_3 + 5.894X_2X_3 - 86.784X_1X_2X_3 \quad (4)$$

The values of t-criteria, as well as adequacy verifications for the model illustrated above, are represented in Table 9.

Strain at maximum load at room temperature, can be seen via encoded values, in Fig.14.

Table 9. Adequacy verification of the strain at maximum load model at 20°C

control points	y	Y'	t_{cal}	A ($t_{cal}<t_{tab}$)
Y112	8.066	10.623	0.76	ADEQUATE
Y113	7.301	10.233	0.88	ADEQUATE
Y122	10.812	11.057	0.07	ADEQUATE
Y133	8.710	9.781	0.32	ADEQUATE
Y223	9.006	10.630	0.48	ADEQUATE
Y233	9.747	9.743	0.00	ADEQUATE
S_y=3.48%	f=7	α=0.05	t_{tab}=2.36	

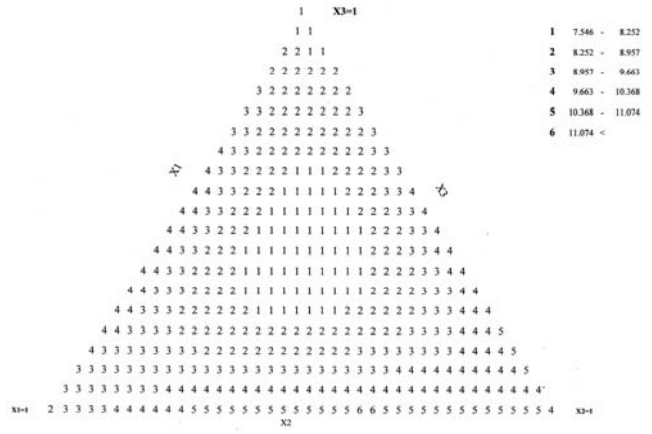

Figure 14. Strain at maximum load levels at 20°C

Strain at maximum load, ε_m, at 20°C ranges from 7.5 % to 11.1% (48 %). What is interesting is that the strain values increase in compositions with all three fractions with the maximum participation of the coarsest AP fraction, and so do the viscosity values, as seen in Figures 14 and 15. On the other hand, trimodal compositions in the centre of the plan in Fig.14 provide the lowest values with the minimum part of the coarsest fraction.

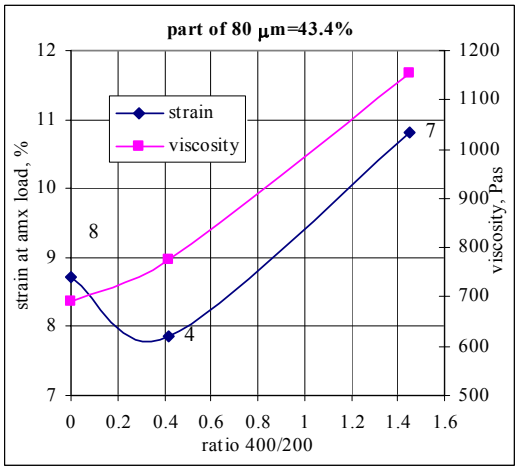

Figure 15. Effect of 400/200 ratio at mas.% 80 μm=43.4=const on the viscosity and the strain at maximum load values

Although uniaxial mechanical properties at extreme temperatures have not been considered by simplex method, tensile strength and strain values at –50°C are noted as the highest ones due to the effects of secondary bonds between the molecules. At lower temperatures, molecules are contracted and they get closer to each other, so the secondary (Coulomb`s) forces are more prominent. By increasing the temperature, molecules separate, enlarging the distance between them and the secondary forces decrease with each square of distance.

Conclusion

Analysing the data obtained using the method of local simplex - lattice planning it has been concluded that the use of selected oxidizer fractions in the high-energy propellants formulations can adjust:

- burning rates within the range of 25 % (from 7.5 mm/s to 9.2 mm/s at 70 bar), with the pressure exponent range of 20 % (from 0.44 to 0.53). The lowest burning rate corresponds the maximum AP fraction limit of 400 μm, and the highest can be expected in compositions with fractions ratio 200 μm: 80 μm as 1:1. The lowest exponent values are obtained for compositions without the coarsest fraction, and the greatest values are characteristic for trimodal compositions with the maximum part of 80 μm;
- tensile strength at room temperature within the range of 33 % (from 0.75 MPa to 1 MPa). The minimum values are obtained for compositions with prevalent participation of two coarser fractions and the maximum values are obtained for trimodal mixture and composition free from 400 μm fraction, the consequence of bonding agent effect and available contact surface;
- strain at maximum load at room temperature within the range of 48 % (from 7.5 % to 11.1 %). The lowest values are the result of trimodal compositions, almost free from the coarsest fraction and equal mass mix of 200 μm and 80 μm AP fractions. Strain values are enhanced when nearly equal fraction ratios are used, i.e. increasing the 400 μm fraction in mixture;
- Viscosity and density values are reversely proportional in bimodal mixtures. By adding the third component, these two values follow each other. Adding the finest fraction to compositions with the minimum participation of 400 μm AP, will cause a great drop of viscosity producing more convenient conditions and density rise.

Composition No.2 with equal portions of fractions of 400 μm and 80 μm shows the best particle packing, from the viscosity viewpoint, satisfactory density values, but low burning rate values due to a great part of 400 μm AP. Therefore, the content of 400 μm has to decrease to about 15 mas.% and 200 μm/80 μm ratio to be kept at 0.7. On the basis of the illustrated analysis, the composition of the lowest viscosity, the best package, maximum burning rate (although higher pressure exponent), as well as the most convenient mechanical properties are found in composition No.10.

The applied method of experiment planning and result processing enables selecting propellants with the desired properties by simply overlapping the obtained diagrams describing the dependence of the measured response and AP fraction.

References

[1] SCHOEYER,H., KORTING,P.: *Low pressure combustion of composite propellant*, Propellants, Explosives, Pyrotechnics 9, 149-156, 1984.

[2] GURDIP, *Burning rate modifiers for composite solid propellants*, J.Scient. Ind. Res.,Vol 37, pp 80, 1978.

[3] TIMNAT,I.: *Raketnie dvigateli na hemičeskom toplive*, "Mir Publishers", Moskva, 1990.

[4] AKHNAZAROVA,A., KAFAROV,V.: E*xperiment Optimization Chemistry and Chemical Engineering*, Mir Publishers, Mo

[5] BAJLOVSKI,M., RODIĆ,V.: *Kompozitna raketna goriva malih brzina sagorevanja*, VTI-004-01-0234, Beograd 2000.

[6] LAZIĆ,Ž.: *Razvojni postupci prenosa proizvodnih uslova u dobijanju čvrstih raketnih goriva*, Doktorska disertacija, TMF, Beograd, 1982.

[7] SNO 7697: *Ispitivanje mehaničkih osobina testom jednoosnog zatezanja "JANAF C" epruveta*

[8] SNO 7695: *Ispitivanje mehaničkih testom jednoosnog zatezanja*

[9] MIL 8462: *Merenje gustine goriva na Moor-ovoj vagi*

[10] DUDUKOVIĆ,B., MILOSAVLJEVIĆ,Đ.: *Planiranje eksperimenta i optimizacija procesa*, IHTM, Centar za tehnoekonomiku i programiranje razvoja, Beograd 1976.

Received: 30.10.2004.

Tromodalna smeša amonijum-perhlorata u kompozitnim raketnim gorivima

U radu su prikazani rezultati ispitivanja sastava kompozitnih raketnih goriva kod kojih je menjan sadržaj tri frakcije amonijum-perhlorata sa srednjim prečnikom čestica od 200 μm, 400 μm i 80 μm. Kao odzivi su mereni brzina sagorevanja i eksponent u zakonu brzine sagorevanja, kao i jednoosne mehaničke karakteristike, a rezultati su obrađeni pomoću lokalnog simpleks – rešetkastog plana nepotpunog trećeg reda.

Ključne reči: **kompozitno raketno gorivo, amonijum perhlorat, brzina sagorevanja, eksponent pritiska, planirani eksperiment, zatezna čvrstoća, izduženje.**

Тройная смесь аммония перхлората в многокомпонентных ракетных топливах

В настоящей работе показаны результаты испытывания состава многокомпонентных ракетных топлив, у которых сделаны изменения содержания трёх частей аммония перхлората со средним диаметром частиц 200 Ем, 400 Ем и 80 Ем. В роли следствия измерены скорость горения и показатель в законе скорости горения (баллистические показатели), а в том числе и одноосные механические характеристики, а результаты того обработаны при помощи местного симплекс-метода - планирования кристаллической решётки неполного третьего ряда.

Ключевые слова: **многокомпонентное ракетное топливо, аммония перхлорат, скорость горения, показатель степени давления, планированный эксперимент, затяжная прочность, удлинение.**

Le mélange trimodal de l'ammonium-perchlorate dans les propergols composites

Les résultats des essais sur la composition des propergols composites chez lesquels on a changé la teneur de trois fractions de l'ammonium-perchloratre au diamètre moyen des particules de 200μm, 400μm et 80μm sont présentés dans cet article. Comme réponse, on a mesuré la vitesse de combustion et l'exposant de la loi de vitesse de combustion ainsi que les propriétés mécaniques uniaxiales. Les résultats obtenus ont été traités à l'aide du plan local simplex treillis des troisièmes séries partielles.

Mots clés: **propergol composite, ammonium-perchlorate, vitesse de combustion, exposant de tension, essai projeté, résistence à la traction, allongement.**